Available online at www.sciencedirect.com
SCIENCE DIRECT®
Journal of Solid State Chemistry 179 (2006) 544–550
JOURNAL OF SOLID STATE CHEMISTRY
www.elsevier.com/locate/jssc

Structural behavior of $Sr_2Bi_2O_5$ at high pressures

F.X. Zhang[a,*], B. Manoun[a], S.K. Saxena[a], C.S. Zha[b]

[a]CeSMEC, Florida International University, University Park, Miami, FL 33199, USA
[b]Cornell High Energy Synchrotron Source, Ithaca, NY 14853, USA

Received 30 June 2005; received in revised form 5 November 2005; accepted 12 November 2005
Available online 20 December 2005

Abstract

The structure of $Bi_2Sr_2O_5$ at high pressures is investigated by in situ X-ray diffraction (XRD) and Raman scattering methods. Raman results indicate that there are two pressure-induced phase transitions that occurred at ~1.4 and ~11 GPa, respectively. XRD measurements reveal only one high-pressure phase, which is indexed with a monoclinic unit cell and the possible space groups are $P121$(No. 3), $P1m1$(No. 6) and $P12/m1$(No. 10). The phase transition above 11 GPa is probably due to the symmetry change without discontinuity of the unit cell. The high-pressure phase is quenchable and it is a new dense form and about 11% denser than the normal orthorhombic $Bi_2Sr_2O_5$ at room conditions.

Keywords: High pressure; Raman; Phase transition

1. Introduction

The phase diagram of the Bi–Sr–O ternary system has been investigated over its entire compositional range [1–3]. Besides the solid solutions of SrO in Bi_2O_3, there are at least five stable ternary phases in the system. The understanding of formation and stability of these phases is important to the investigation of the multicomponent Bi–Sr(–Ca)–Cu–O system, where several superconducting phases are found [4–6]. The Bi–Sr–O ternary system is also of interest in electroceramic applications because of the high oxygen conductivity of δ-Bi_2O_3 [7] and the rhombohedral β-phase. Recently, some oxides in the system, such as Bi_2CaO_4, have been found to be ecomaterials and efficient photocatalysts in decomposing organic contaminations [8].

The previous experimental results at normal pressure generally reveal that the orthorhombic $Bi_2Sr_2O_5$ is stable up to 1200 K [9,10], but the unit cell and structural details have some disagreement in the literature [11,12]. X-ray crystallography gave a space group of *Pnma* for $Bi_2Sr_2O_5$ and the X-ray diffraction measurements resulted in cell dimensions of 14.3019, 6.1718 and 7.6524 Å [11]. The combined XRD and neutron diffraction resulted in cell dimensions of 3.8268, 14.3142 and 6.1724 Å and space group of *Cmcm* [12]. The lattice parameter c of the first unit cell is double of parameter a of the latter one and the other two cell parameters have very close values, so the first unit cell seems to be a commensurate superlattice of the latter one. In fact, the atomic bonding environment in the above two structure models is different.

The phase stability of $Bi_2Sr_2O_5$ at high temperatures was studied before. The high-temperature XRD investigations revealed that $Bi_2Sr_2O_5$ transformed to γ-Bi_2O_3 and $Bi_2Sr_3O_6$ above 1213 K [9] or melt incongruently [10]. The high-pressure behavior of alkaline-earth oxide binary systems have been widely studied both experimentally and theoretically because of their wide range of applications as catalysts and refractory ceramics. In addition, some similar oxides, such as CaO, are important constituents of the earth's lower mantle. The NaCl-type structure of SrO has also been found to transform to CsCl-type structure at 36 GPa [13–15]. A pressure-induced amorphization was confirmed by Raman scattering measurements in Bi_2O_3 [16]. For the quarternary system BiSrCuO, high pressure is a good method for the synthesis of superconductor phases [6]. However, as far as we know, there is no report on the structural studies in the Bi–Sr–O ternary system at high

*Corresponding author. Fax: +305 3483070.
E-mail address: zhangf@fiu.edu (F.X. Zhang).

0022-4596/$ - see front matter © 2005 Elsevier Inc. All rights reserved.
doi:10.1016/j.jssc.2005.11.018

pressures up to now. In this paper, the structural behavior of $Bi_2Sr_2O_5$ at high pressures up to 41.5 GPa was studied and pressure-induced phase transitions were detected by in situ XRD and Raman scattering methods.

2. Experimental section

The $Bi_2Sr_2O_5$ compound is synthesized by solid-state reaction in air. Well mixed powders of Bi_2O_3 (99.5%, Alfa Aesar Ltd.) and SrO (99%, Alfa Aesar Ltd.) with nominal composition of $Bi_2Sr_2O_5$ were pressed into pellets and heated up to 1073 K for 96 h with intermediate grinding. XRD measurements confirmed the single orthorhombic structure for the final product and the XRD pattern is refined with the Rietveld method through program Fullprof [17]. Pressure was generated with diamond anvil cell (DAC) techniques using stainless steel gaskets for both XRD and Raman measurements. The in situ high-pressure XRD measurements were performed with synchrotron radiation X-ray source (0.486 Å) at Cornell High Energy Synchrotron Source (CHESS). The Bragg diffraction images were recorded with a CCD detector (MAR 345) in transmission mode and the XRD patterns were integrated from the images with FIT2d software. The XRD peaks are fitted individually and the unit cell is indexed by the least-square method with program Dicvol [18]. Raman spectra were collected by using a high throughput holographic imaging spectrograph with volume transmission grating, holographic notch filter and a thermoelectrically cooled CCD detector (Physics Spectra). The light is 783.54 nm in wavelength from a He–Ne laser and the laser power is controlled below 5 mW. Our experiments find that $Bi_2Sr_2O_5$ sample is a very soft material and the bulk modulus is comparable with Al, which we used as a pressure media before [19]. The phase transition in $Bi_2Sr_2O_5$ occurred at quite low pressure (starting at 1.4 GPa), so the non-hydrostatic condition has no big effect on our results. The pressure in all the experiments was measured by the ruby fluorescence method [20] and the pressure difference between the center and near the edge of the sample chamber in our experiments is less than 5 GPa when the pressure is higher than 30 GPa.

3. Results and discussions

As described above, $Bi_2Sr_2O_5$ is orthorhombic and at least two sets of unit cell and space group are reported before [10,11]. The synchrotron XRD pattern of the synthesized $Bi_2Sr_2O_5$ at normal pressure can be indexed with a pure orthorhombic phase. Our structural model is comparable with that in Ref. [11]. Rietveld refinement based on space group of *Cmcm* and lattice parameters $a = 3.8054(5)$ Å, $b = 14.232(3)$ Å, $c = 6.139(1)$ Å results in a good fit between the observed and calculated XRD patterns (Fig. 1). Fig. 2 is the schematic crystal structure of $Bi_2Sr_2O_5$. It is a layered structure, which contains four

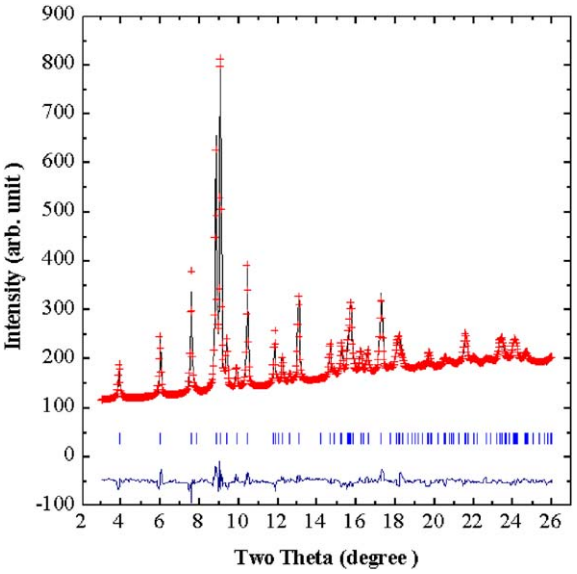

Fig. 1. The XRD pattern of the orthorhombic $Bi_2Sr_2O_5$ phase and its refinement results. Lattice constants: $a = 3.8054(3)$ Å, $b = 14.232(3)$ Å, $c = 6.139(1)$ Å, space group: *Cmcm*, residues: $R_p = 2.05\%$, $R_{wp} = 2.82\%$, $R_{Bragg} = 7.81\%$.

layers along the long *b*-axis and can be written as $ABB'A'$. Layers *A* and *B* are center reversed with layers A' and B', respectively. The Bi ions, in fact, are only 3 coordinated with oxygen because O2 only has half occupancy. The Sr atoms have four closer neighboring oxygen atoms in the same layer and another two in the neighbor layers, which has a longer bonding distance. (Sr–O: 2.527 Å, 2.597 Å in *A*–*B* and *B*–*B'* layers, respectively).

There are 4 independent atoms in the unit cell of $Bi_2Sr_2O_5$ and the Wyckoff positions are 4*c* (Bi, Sr, O1) and 8*f* (O2). Thirty Raman active modes are predicted at the center of Brillouin zone according to group factor analysis:

$$\Gamma = 5A_g + 4B_{1g} + B_{2g} + 5B_{3g}.$$

Fig. 3 shows the measured Raman spectrum of $Bi_2Sr_2O_5$ at different pressures. At normal pressure, at least 10 Raman modes are clearly observed. As far as we know, this is the first report on the Raman spectrum of $Bi_2Sr_2O_5$ and it is not easy to make a quantitative assignment for these observed modes. However, from the analysis of the previous experimental observations in α-Bi_2O_3 [16,21] and other Bi-contained oxides [22–24], we believe that the modes with shift below 400 cm^{-1} are related to the Bi–O bonds in the compound. The two modes centered at 560 and 650 cm^{-1} at normal pressure are attributed to the Sr–O bond. A mode with a similar frequency was also observed in multi-component superconductors of $Bi_2Sr_{2-x}La_xCuO_{6+d}$ [22,23] and BiPbSrCuO [24]. With increase of pressure, the mode centered at 650 cm^{-1} with a strong intensity at normal pressure loses its intensity gradually and a new mode around 570 cm^{-1} starts to appear when the pressure is increased to 1.4 GPa. This means that a pressure-induced

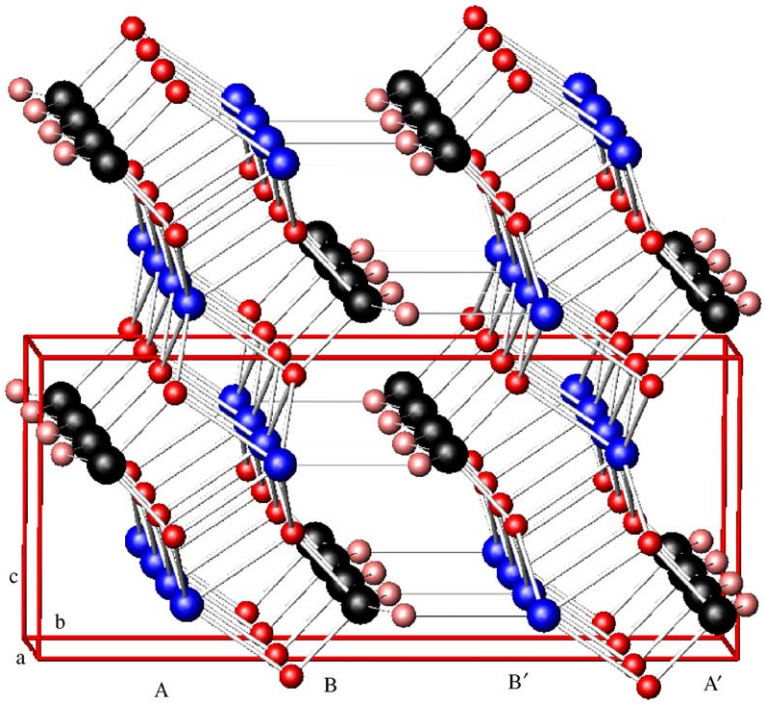

Fig. 2. Schematic crystal structure of $Bi_2Sr_2O_5$ at normal conditions. The biggest atoms are Bi and the smallest ones are oxygen.

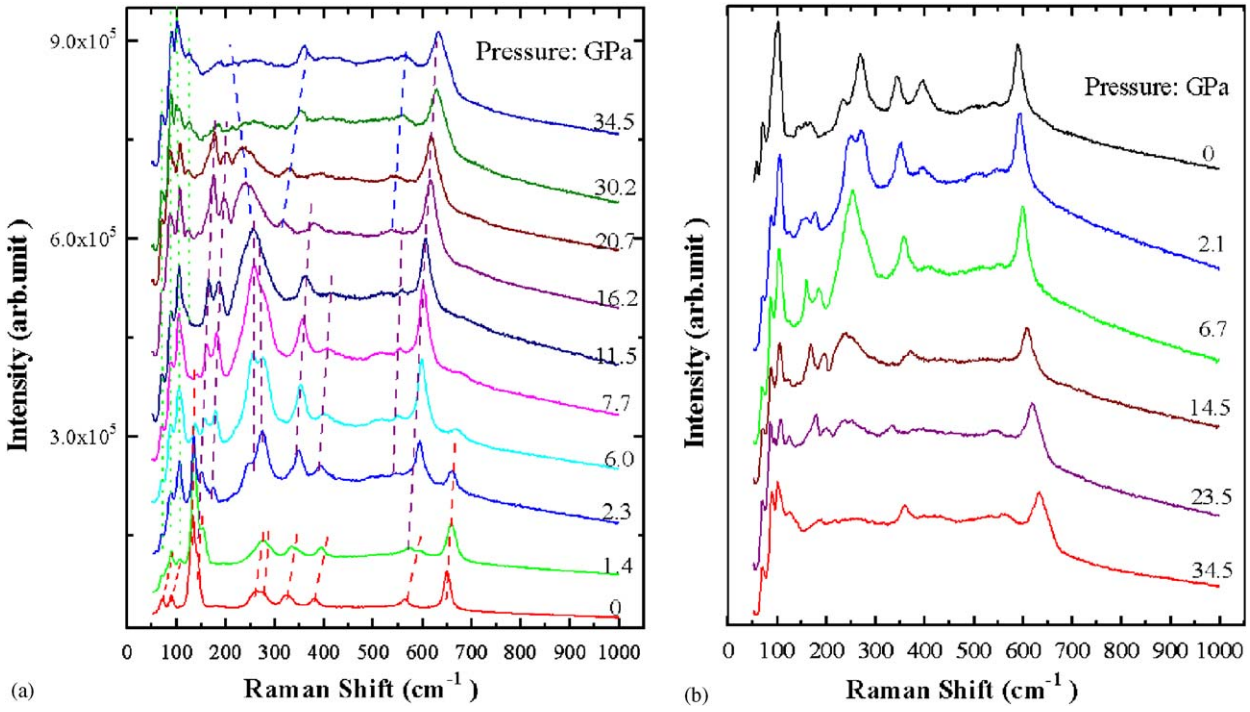

Fig. 3. (a) Evolution of Raman spectra of $Bi_2Sr_2O_5$ at different pressures, (b) Raman spectra of $Bi_2Sr_2O_5$ measured during pressure release.

phase transition occurs at pressure as low as 1.4 GPa. The two most intense modes of the normal $Bi_2Sr_2O_5$ phase centered at 130 and 650 cm^{-1} disappeared completely after 7.7 GPa, so the pressure-induced phase transition is completed at this pressure based on the Raman measurements. In the orthorhombic $Bi_2Sr_2O_5$, the bonding distance between Sr and O atoms between different layers is 2.597 Å, which is longer than the Sr–O distance in the same layers

(2.527 Å). The XRD results below indicate that the space between layers is greatly compressed at high pressures. The bonding of Sr and O atoms between neighboring layers is strengthened and the bonding environment of O is changed at high pressures. That is why the high-frequency modes related to O(Sr) in the orthorhombic phase completely changed after the phase transition. The Raman spectrum shows no new peaks appearing in our measurement until 16.2 GPa. After 16.2 GPa, two weak additional modes appeared in the spectrum centered at ~310 and 530 cm^{-1}. This indicates that another phase transition takes place at this pressure. The wide band at around 250 cm^{-1} for the high-pressure phase, which is composed of several Raman active modes, shifts to lower frequencies and loses intensity gradually with increasing pressure. These modes have strong relation with the Bi–O bonds. At higher pressure, the oxygen (O2) may bond with Bi in the neighboring layer to form a three-dimensional network, so the bonding environment of Bi ions has great changes in the high-pressure phase.

The bands below 100 cm^{-1} at high pressures are not distinguishable from the laser light in our experimental setup. Fig. 3b shows the evolution of the Raman spectrum during the unloading process. The two strongest modes centered at 130 and 650 cm^{-1} in the normal phase are not found in the quenched sample. Though there is a weak band at around 130 cm^{-1} in the spectrum of the quenched sample, it is a different mode from the normal phase because of the weak intensity. The Raman spectrum of the quenched sample shows a similar character with those of the high-pressure phase (pressure less than 11.5 GPa), so the high-pressure phase is quenchable. The pressure dependence of Raman shift is plotted in Fig. 4. Two phase transitions are clearly observed—the normal phase (I) of $Bi_2Sr_2O_5$ first transforms to high-pressure phase (II) at less than 2 GPa. After 11.5 GPa, another high-pressure phase (III) appeared. After releasing pressure, it transforms to high-pressure phase (II).

In order to confirm the above phase transitions observed in the Raman observations, in situ XRD experiments were performed from normal pressure to 41.5 GPa. Fig. 5 shows the evolution of XRD patterns with pressure. The XRD pattern starting at 3.8 GPa is quite different from the pattern at normal pressure. A strong peak at 9.8° appeared and the peak at 10.4° and some weak diffraction peaks in the pattern at normal pressure disappeared. The diffraction peaks at 3.8 GPa cannot be indexed with the orthorhombic unit cell, however, with program Dicvol [18], the 14 main diffraction peaks can be indexed by a monoclinic unit cell with lattice parameters of 6.39, 3.643, 6.16 Å and β angle of 90.2° (Table 1), resulting in $M(14) = 22.7$. All the diffraction peaks at other high pressures can also be indexed with a similar monoclinic unit cell. The agreement gives us confidence for the above indexing results. Unlike Raman results, XRD patterns did not show the coexistence of the normal phase and high-pressure phase. Raman scattering measurements reflects local atomic structure and is more sensitive to phase identifications than the XRD measurement. Such as our recent work [19] on pyrochlore $Sm_2Ti_2O_7$, Raman measurements found a complete disordered state at 40 GPa, but XRD patterns still show a crystalline state till to 51 GPa.

With increase of pressure, the two peaks at ~9° first split and overlapped completely between 11 and 20 GPa and

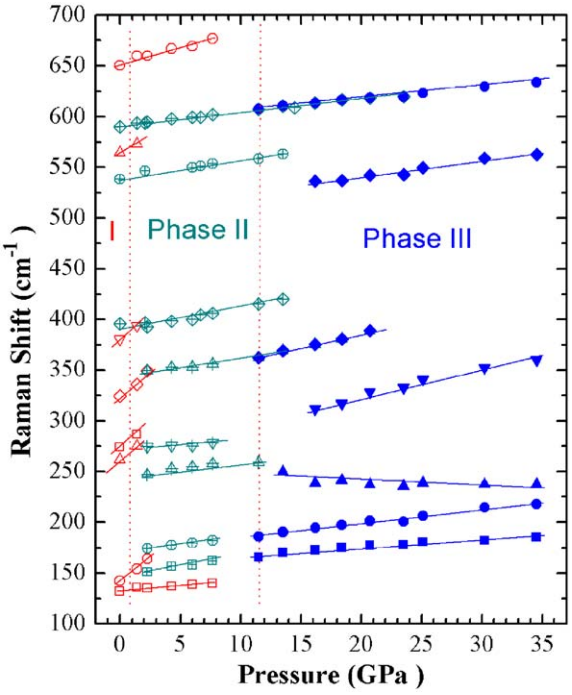

Fig. 4. Pressure dependence of the Raman shifts for $Bi_2Sr_2O_5$.

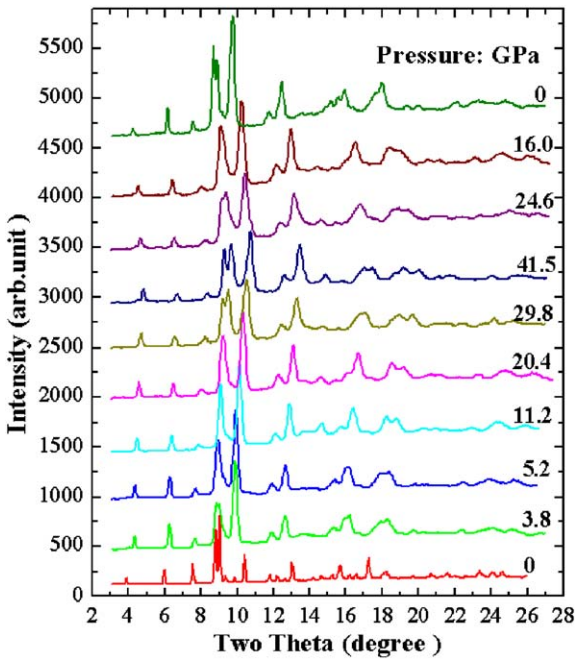

Fig. 5. XRD patterns of $Bi_2Sr_2O_5$ at different pressures.

Table 1
Indexed results of $Bi_2Sr_2O_5$ at 3.8 GPa with monoclinic unit cell

$h\,k\,l$	$d_{obs.}$ (Å)	$d_{cal.}$ (Å)	$d_{obs.}-d_{cal.}$ (Å)
1 0 0	6.4114	6.3943	0.0171
1 0 $\bar{1}$	4.4420	4.4456	−0.0036
1 0 1		4.4284	0.0136
0 1 0	3.6342	3.6432	−0.0090
1 1 0	3.1570	3.1655	−0.0084
0 0 2	3.0908	3.0808	0.0099
1 1 $\bar{1}$	2.8187	2.8178	0.0009
1 1 1		2.8134	0.0053
0 1 2	2.3449	2.3525	−0.0076
1 1 $\bar{2}$	2.2083	2.2099	−0.0016
1 1 2		2.2057	0.0026
0 2 0	1.8253	1.8216	0.0037
3 0 $\bar{2}$	1.7560	1.7560	0.0000
1 1 $\bar{3}$	1.7246	1.7245	0.0001
1 1 3		1.7215	0.0031
2 0 3		1.7250	−0.0004
2 1 $\bar{3}$	1.5603	1.5636	−0.0033
2 1 3		1.5591	0.0012
2 2 $\bar{1}$	1.5299	1.5337	−0.0038
2 2 1		1.5323	−0.0023
0 1 4	1.4189	1.4188	0.0001
4 0 $\bar{2}$		1.4212	−0.0023
4 0 2		1.4167	0.0022

a=6.39(5) Å, b = 3.643(8) Å, c=6.16(2) Å, β = 90.2(7)°, V=143.5(2) Å^3.

Table 2
Indexed results of $Bi_2Sr_2O_5$ at 20.4 GPa with monoclinic unit cell

$h\,k\,l$	$d_{obs.}$ (Å)	$d_{cal.}$ (Å)	$d_{obs.}-d_{cal.}$ (Å)
1 0 0	6.0754	6.0418	0.0336
1 0 $\bar{1}$	4.2980	4.2865	0.0116
0 1 0	3.4712	3.4748	−0.0036
2 0 0	3.0211	3.0209	0.0002
1 0 $\bar{2}$	2.7011	2.7040	−0.0029
1 1 $\bar{1}$		2.6993	0.0018
0 1 2	2.2746	2.2736	0.0010
1 1 $\bar{2}$	2.1314	2.1340	−0.0026
3 0 $\bar{1}$	1.9140	1.9162	−0.0022
2 1 2	1.8123	1.8091	0.0031
0 2 0	1.7372	1.7374	−0.0002
3 1 $\bar{1}$	1.6749	1.6780	−0.0031
1 1 $\bar{3}$		1.6731	0.0018
4 0 0	1.5085	1.5104	−0.0019
2 2 0		1.5061	0.0024
4 0 1	1.4589	1.4610	−0.0022
2 2 1		1.4590	−0.0001
1 2 2		1.4578	0.0012
4 1 $\bar{1}$	1.3530	1.3530	0.0000
0 0 5	1.2020	1.2026	−0.0007
2 2 3		1.2008	0.0012
3 2 2		1.2019	0.0000
3 1 4	1.1320	1.1327	−0.0007
4 2 $\bar{2}$	1.0693	1.0689	0.0004

a=6.042(6) Å, b=3.475(4) Å, c=6.01(1) Å, β = 90.7(1)°, V = 126.3(2) Å^3.

then split again after that. According to the Raman measurements, there should be another phase transition at or after 11.5 GPa. However, all the diffraction peaks of high-pressure XRD patterns can be indexed with the similar monoclinic unit cell in the whole measured pressure range. We do find an additional weak peak at around 14.5° in the patterns after 11.2 GPa, but it can be indexed with the (30$\bar{1}$) diffraction in the monoclinic unit cell. Table 2 gives the indexed results of XRD pattern at 20.4 GPa.

There is no obvious extinction rules in the indexed results, so three possible space groups are expected for the monoclinic high-pressure phase: $P121$ (3), $P1m1$ (6) and $P12/m1$ (10). We believe that the phase transition of II–III in the Raman observation may be caused by space group change without any discontinuity change of the unit cell. Figs. 6a,b show the pressure dependence of the cell parameters of the high-pressure phase. The longest cell parameter has a large slope with pressure, so the unit cell is easier to be compressed along the (100) direction. The Sr and O atoms in neighboring layers will bond directly at high pressures. The new high-pressure phase is a dense form of $Bi_2Sr_2O_5$. The calculated cell volume per formula of $Bi_2Sr_2O_5$ of the high-pressure phase at normal pressure is only 90% of the normal phase. The XRD pattern of the quenched sample is same with that taken at 3.8 GPa, so the high-pressure phase II is quenchable to room conditions.

The pressure dependence of the unit cell volume for the high-pressure phase is plotted in Fig. 6c. Ignoring the discontinuity of cell volume during phase transitions, fit with Birch–Murnaghan equation yields quite a low value of the bulk modulus 71(9) GPa and the first pressure derivative of the bulk modulus $B' = 4.9(9)$ for the high-pressure phase of $Bi_2Sr_2O_5$. The bulk modulus is comparable with that of Al and $Bi_2Sr_2O_5$ is thus a very "soft" ceramic material.

4. Conclusions

A pressure-induced phase transition from the orthorhombic to monoclinic structure in the ternary compound $Bi_2Sr_2O_5$ was found by in situ Raman scattering and XRD measurements. The phase transition is irreversible and the high-pressure phase is quenchable to room conditions. The unit cell is much compressed between different layers and Sr and O atoms in different layers bond directly forming a three-dimensional network at high pressures. The oxide of $Bi_2Sr_2O_5$ is a very "soft" ceramic material and the new high-pressure phase is about 11% denser than the normal phase at room conditions.

Acknowledgments

This work was financially supported by grants from the National Science Foundation (DMR-0231291,

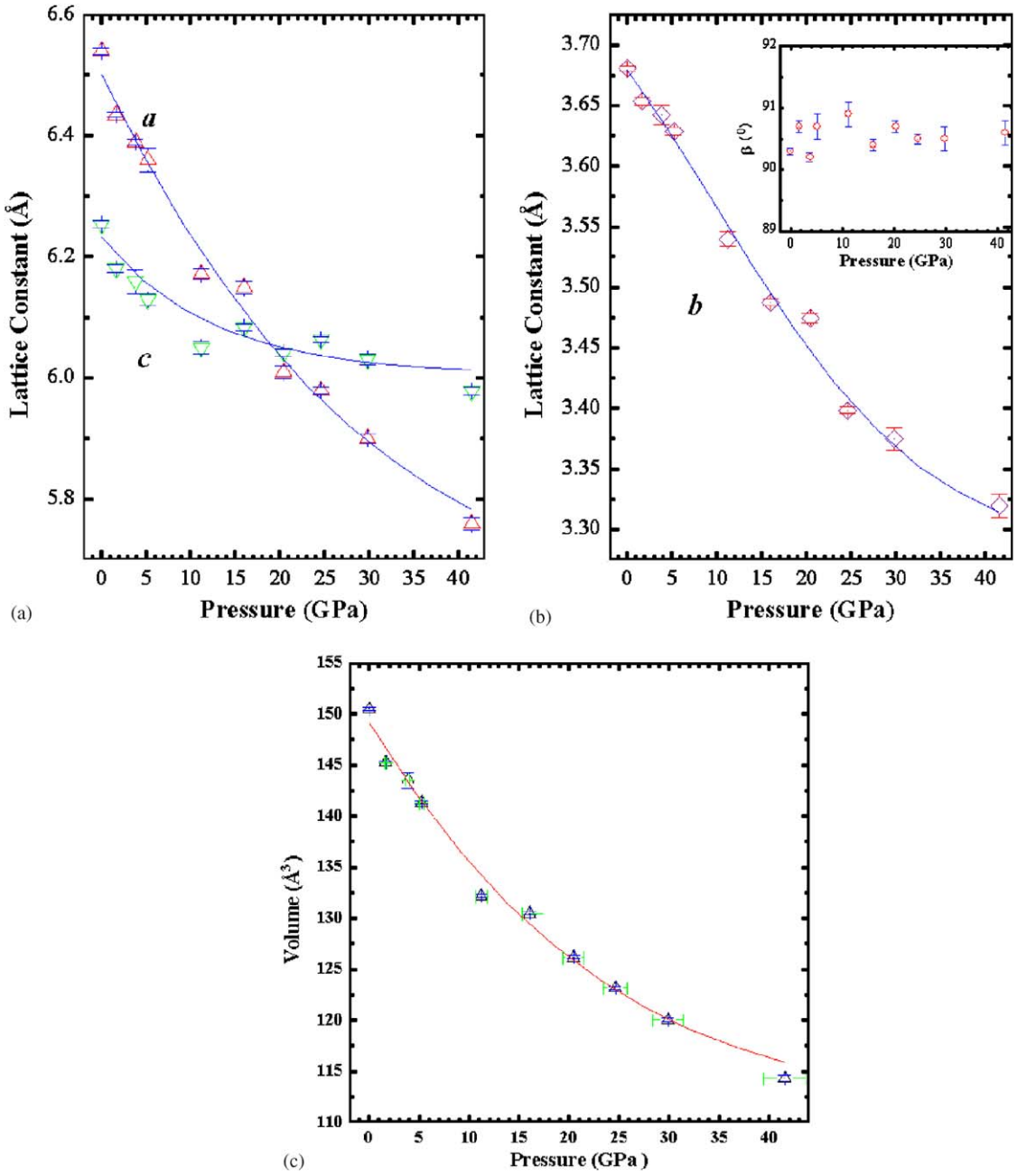

Fig. 6. Pressure dependence of the indexed cell parameters (a), (b) and cell volume (c) of the new high-pressure phase of $Bi_2Sr_2O_5$.

EAR-00769641). The XRD work is based upon research conducted at the Cornell High Energy Synchrotron Source (CHESS), which is supported by the National Science Foundation under award DMR -0225180.

References

[1] N.M. Hwang, R.S. Roth, C.J. Rawn, J. Am. Ceram. Soc. 73 (1990) 2531.
[2] F. Abbattista, C. Brisi, D. Mazza, M. Vallino, Mater. Res. Bull. 26 (1991) 107.
[3] R.S. Roth, C.J. Rawn, B.P. Burton, F. Beech, J. Res. Natl. Inst. Stand. Technol. 95 (1990) 291.
[4] B. Hallstedt, D. Risold, L.J. Gauckler, J. Am. Ceram. Soc. 80 (1997) 1085.
[5] P. Majewski, Adv. Mater. 6 (1994) 460.
[6] A. Ono, S. Horiuchi, M. Tsutsumi, Physica C 226 (1994) 360.
[7] T. Takahashi, H. Iwahara, Mater. Res. Bull. 13 (1978) 1447.
[8] J.W. Tang, Z.G. Zou, J.H. Ye, Angew. Chem.—Int. Ed. 43 (2004) 4463.
[9] P. Conflant, M. Drache, T.P. Wignacourt, J.C. Boivin, Mater. Res. Bull. 26 (1991) 1219.
[10] E. Yu Vstavskaya, A. Yu Zuev, V.A. Cherepanov, S.D. Sutton, J.S. Abell, J. Phase Equilib. 15 (1994) 573.

[11] C.C. Torardi, J.B. Parise, A. Santoro, C.J. Rawn, R.S. Roth, B.P. Burton, J. Solid State Chem. 93 (1991) 228.
[12] J.F. Vente, R.B. Helmholdt, D.J.W. Ijdo, Acta Crystallogr. C 48 (1992) 1380.
[13] Y. Sato, R. Jeanloz, J. Geophys. Res. 86 (1981) 11.
[14] Y. Sato, R. Jeanloz, J. Geophys. Res. 86 (1981) 773.
[15] G. Kalpana, B. Palanivel, M. Pajagopalan, Phys. Rev. B 52 (1995) 4.
[16] C. Chouinard, S. Desgreniers, Solid State Commun. 113 (2000) 125.
[17] J. Rodrguez-Carvajal, FULLPROF, Version 2k, 2001.
[18] A. Boultif, D. Louer, J. Appl. Crystallogr. 24 (1991) 987.
[19] F.X. Zhang, B. Manoun, S. Saxena, C.S. Zha, Appl. Phys. Lett. 86 (2005) 181906.
[20] H.-K. Mao, J. Xu, P.M. Bell, J. Geophys. Res. 91 (1986) 4672.
[21] V.N. Denisov, A.N. Ivlev, A.S. Lipin, B.N. Mavrin, V.G. Orlov, J. Phys.: Condens. Matter 9 (1997) 4967.
[22] O.M. Osada, M. Kakihana, M. Kall, L. Borjesson, A. Inoue, M. Yashima, Phys. Rev. B 56 (1997) 2847.
[23] C.V.N. Rao, H.J. Trodahl, J.L. Tallon, Physica C 251 (1994) 192.
[24] H. Yan, Z. Mao, G. Xu, Y. Zhang, Phys. Rev. B 59 (1999) 8459.